Dissecting DNA-Histone Interactions in the Nucleosome by Molecular Dynamics Simulations of DNA Unwrapping

Ramona Ettig,[†] Nick Kepper,[†] Rene Stehr,[‡] Gero Wedemann,[‡] and Karsten Rippe[†*]
[†]Deutsches Krebsforschungszentrum (DKFZ) and BioQuant, Research Group Genome Organization & Function, Heidelberg, Germany; and [‡]University of Applied Sciences Stralsund, Competence Center Bioinformatics, Stralsund, Germany

ABSTRACT   The nucleosome complex of DNA wrapped around a histone protein octamer organizes the genome of eukaryotes and regulates the access of protein factors to the DNA. We performed molecular dynamics simulations of the nucleosome in explicit water to study the dynamics of its histone-DNA interactions. A high-resolution histone-DNA interaction map was derived that revealed a five-nucleotide periodicity, in which the two DNA strands of the double helix made alternating contacts. On the 100-ns timescale, the histone tails mostly maintained their initial positions relative to the DNA, and the spontaneous unwrapping of DNA was limited to 1–2 basepairs. In steered molecular dynamics simulations, external forces were applied to the linker DNA to investigate the unwrapping pathway of the nucleosomal DNA. In comparison with a nucleosome without the unstructured N-terminal histone tails, the following findings were obtained: 1), Two main barriers during unwrapping were identified at DNA position ± 70 and ± 45 basepairs relative to the central DNA basepair at the dyad axis. 2), DNA interactions of the histone H3 N-terminus and the histone H2A C-terminus opposed the initiation of unwrapping. 3), The N-terminal tails of H2A, H2B, and H4 counteracted the unwrapping process at later stages and were essential determinants of nucleosome dynamics. Our detailed analysis of DNA-histone interactions revealed molecular mechanisms for modulating access to nucleosomal DNA via conformational rearrangements of its structure.

INTRODUCTION

The nucleosome is the fundamental unit of chromatin in eukaryotes (1). It contains two copies each of histone proteins H2A, H2B, H3, and H4, and 146/147 basepairs (bp) of DNA (1,2). The DNA stably contacts the surface of the histone protein octamer core in a left-handed superhelix of almost two turns. Histone proteins consist of a globular part formed by three well-structured α-helices and the histone tails. These are long protruding N-terminal or, in the case of histone H2A, C-terminal extensions that lack secondary structure and adopt variable conformations. Removal of the histone tails leads to some increase of nucleosome flexibility and affects the binding of other proteins to the nucleosome and/or its associated DNA (3–5). The interactions of the unstructured histone N-terminal tails are modulated by posttranslational modifications like acetylation, methylation, and phosphorylation at numerous sites mostly in H3 and H4. These are set or removed in a dynamic manner by specific enzymes (6,7). Histone tails can serve as binding sites for protein domains that specifically interact with the posttranslationally modified histone state. In addition, acetylation of histone lysines has a direct effect on the stability of the nucleosome core particle, and on its higher-order interactions because the positively charged lysine is neutralized in the acetylated state (8).

The dynamics of the nucleosome in terms of spontaneous DNA unwrapping or breathing were studied by various approaches. It was investigated both experimentally and theoretically how proteins like restriction enzymes or RNA polymerases can access nucleosomal DNA and depend on the spontaneous unwrapping of DNA (9–11). The transition between the closed and partially or fully unwrapped open state was dissected in a number of single-molecule studies (12–15). These yielded lifetimes of several seconds for the closed state that were interrupted by open periods of a few tenths of a second, in which up to 80 bp of nucleosomal DNA were exposed. Finally, the unwrapping of nucleosomal DNA is also a crucial part of the activity of a specific class of enzymes referred to as remodeling complexes. They mediate the ATP-dependent translocations of nucleosomes along the DNA via formation of a DNA loop that is propagated around the histone octamer to change the translational position of the nucleosome (16,17). Thus, understanding the energetics of the DNA interaction with the histone octamer is essential for dissecting cellular processes that control unwrapping of nucleosomal DNA and nucleosome positioning. The strength of the interaction between the DNA and histone protein can be directly investigated in force spectroscopy experiments (18–23).

To relate the experimentally observed nucleosome dynamics with its high-resolution structure, all-atom molecular dynamics (MD) studies are ideally suited (24–27). They allow for a detailed comparison of free DNA with DNA bound to the histone octamer, and an analysis in terms of dynamic DNA double helix features and superhelix configuration (24,26,28). MD studies of systems in the size of the nucleosome already require large computational resources for simulations of tens of nanoseconds. However, with respect to nucleosome dynamics, many processes occur at the microsecond to second timescale (13,15). By applying

an external force in so-called steered molecular dynamics (SMD) simulations, the transition of the system into a certain state can be induced and compared to results from single-molecule force spectroscopy experiments (29–31). Here, we have performed all-atom MD and SMD simulations of a solvated nucleosome with and without the N-terminal histone tails to investigate the process of unwrapping DNA from the histone octamer. Our findings reveal details of the dynamic protein-DNA interactions at atomic resolution that govern the accessibility of nucleosomal DNA. This has a number of implications for the competitive binding of transcription factors to DNA sites occupied by a nucleosome.

MATERIALS AND METHODS

MD and SMD simulations were based on the structure of nucleosome and linker DNA in the tetranucleosome crystal structure 1ZBB (32) that had undergone minimization and had been solvated and equilibrated for 2 ns or 50 ns (33) (see structure NUC, Fig. S1 *A*, in the Supporting Material). For simulations of the tailless nucleosome structure the N-terminal tails were removed from the 50-ns equilibrated complete nucleosome structure so that only amino acids 41–135 (H3), 25–102 (H4), 17–128 (H2A), and 32–122 (H2B) remained (structure NUCΔtail). DNA sequence effects were studied in comparison to an additional nucleosome crystal structure with an adenine $dA_{16} \cdot dT_{16}$ insert (based on coordinates PDB 2fj7, and termed structure NUC_A_{16}) In addition, a structure referred to as NUC_loop was evaluated that had a central DNA loop of 20 bp (see Fig. S1 *B*). Simulations were conducted with the NAMD 2.6 (34) and AMBER 10.0 (35) software packages. Details of the MD and SMD simulations and data analysis are described in the Methods section in the Supporting Material.

RESULTS

DNA-histone interactions occur with a five-nucleotide periodicity

To investigate the interactions between DNA and histone proteins at high resolution, we conducted two MD simulations over a time of ~20 ns in explicit water at physiological concentrations of monovalent ions. In Fig. 1 *A*, the corresponding time-dependent DNA-histone interactions are shown. Additionally, the dynamics of DNA-histone contacts during a 120-ns MD simulation of a nucleosome structure with an internal DNA loop were investigated (see Fig. S2). For the NUC structure, the Fourier spectrum of the time-averaged interactions of the histone octamer and the DNA sequence was calculated (Fig. 1 *B*). It revealed a peak at 0.19/bp, corresponding to a ~5.1-bp periodicity (Fig. 1 *C*). When evaluating the interactions of the two DNA strands of the double-helix separately, a ~10-nucleotide periodicity for each DNA strand with a ~5.5-nucleotide phase shift between the strands was apparent. Thus, contacts of the histone protein core with nucleotides occur with alternating DNA strands. To study effects of the DNA sequence on the observed periodicity, the Fourier spectra of a nucleosome with an insert of dA_{16} at bp −35 was also calculated. This yielded the same results for the interaction periodicity, albeit with weaker histone-DNA interactions in the region of the adenine tract (see Fig. S3).

Histone tail interactions stabilize the nucleosome and can cause an asymmetric DNA interaction pattern

The images in Fig. 1 *A* illustrate the temporal evolution of interactions between DNA and histone proteins. From a comparison of the complete nucleosome with a nucleosome without the N-terminal histone tails, the contribution of the tails can be extracted. As expected, the interactions between DNA and the globular parts of the histone octamer were symmetric relative to the dyad axis. However, due to the variability of contacts made by the flexible tails, the interaction pattern became asymmetric. Thus, factors that direct the histone tails to certain DNA contact regions could induce a preference for unwrapping from one linker DNA side. It appears likely that the tail-DNA interaction pattern will become symmetric on longer timescales due to sampling over the different conformations. However, on the 100-ns timescale, no large rearrangements of the histone tails were observed in the MD simulation (Fig. 1 *A*, and see Fig. S2). The only exception was a relocation of the H2A C-terminus that is depicted in Fig. S4. The spontaneous opening of the DNA-histone interactions at the entry-exit site of the DNA in the nucleosome as well as at the start/end of the looped region comprised only 1–2 bp during the observation period (Fig. 1 *A*, and see Fig. S2, Fig. S5, Fig. S6, and Movie S1 in the Supporting Material).

Unwrapping nucleosomal DNA by applying an external force reveals five phases of DNA unwrapping with two main energy barriers at ±70 bp and ±45 bp

To investigate the unwrapping of DNA from the histone octamer, SMD simulations were conducted. One end of the nucleosomal DNA was fixed, and a harmonic potential moving at constant velocity was applied to the opposite DNA end (Fig. 2). Due to the limitations of the available computational resources, the SMD simulations had to be conducted at a speed that was several orders of magnitude higher than those used in the experimental setups that operate at ~0.1 μm/s. Nevertheless, as discussed in the context of other SMD studies, important information on the most relevant energy barriers as well as the reaction pathway can be derived despite this limitation (29,36–38). The application of the SMD approach to dissect the DNA unwrapping process from the nucleosome identified five characteristic phases and two main energy barriers (Figs. 2 and 3, and see Movie S2 and Movie S3).

Phase I: bending of linker DNA

At the entry-exit site of the nucleosome, the DNA became bent into the direction of applied forces. Without breaking contacts with the histone residues, the nucleosome aligned and the DNA elongated by rearranging bases (tilting and
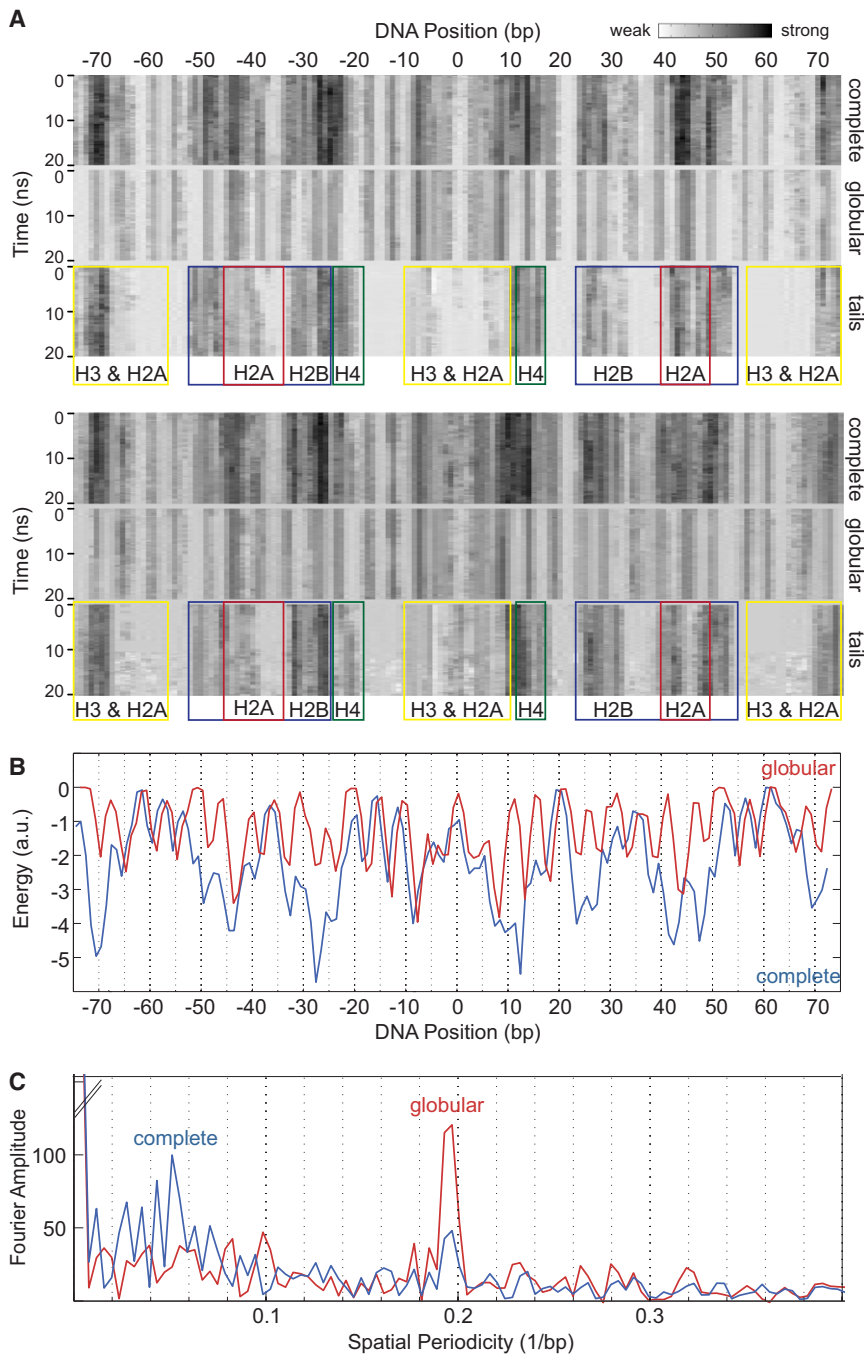
FIGURE 1 High resolution DNA-histone interaction maps. (*A*) Temporal evolution of the histone-DNA electrostatic and van der Waals interactions in a nucleosome calculated for two 20-ns MD simulation trajectories. The interaction strength increases (from *white* to *black*). The DNA position numbering refers to the central base pair 0 at the nucleosomal dyad axis. The three panels in each of the two MD simulations differ with respect to the histone residues that were taken into account for calculating interaction energies with the DNA. They show the complete nucleosome (complete, *top panel*), the interactions without the N-terminal tails (globular, *middle panel*), and the isolated tail contributions (tails, *bottom panel*). The colored boxes indicate the specific histones that are involved in the DNA interactions in this region (H3 and C-terminal H2A, *yellow*; N-terminal H2A, *red*; H2B, *blue*; and H4, *green*). The first MD simulation shown (*top panel*) was conducted with a start configuration of a nucleosome that was derived from the crystal structure (32) but had been already equilibrated for 50 ns (33). The nucleosome start structure of the second MD simulation shown (*bottom panel*) was derived from the same crystal structure, minimized, and equilibrated for only 2 ns. (*B*) The temporal mean energy values of histone-DNA interactions for the entire MD simulation trajectory are plotted with respect to the DNA position for the complete (*blue line*) and the tailless (*red line*) nucleosome. Relative to the nucleosome dyad axis, the red line was much more symmetric than the blue one, demonstrating that the histone tails have a strong influence on the interaction pattern and the interaction symmetry within the nucleosome. (*C*) Fourier spectra for complete and tailless nucleosome interaction maps calculated with the data from panel *B*. When the unstructured histone tails were excluded, a pronounced frequency peak appeared at 0.19/bp that corresponds to a 5.1-bp spatial periodicity.

untwisting). Interactions of the globular histones and the DNA at position ±70 bp were enhanced by binding of the C-terminal H2A and N-terminal H3 tails. These defined a first barrier toward unwrapping.

Phase II: unwrapping of the outer DNA turn

Upon further DNA unwrapping, the barrier at ±70 bp was broken and DNA segments were released in ~5 bp steps until almost the entire outer DNA turn dissociated from the histone octamer core. The outer turn comprised ~67 bp, i.e., the region from ±73 bp to ±40 bp.

Phase III: protein core rotation

To enable further DNA unwrapping, the protein core rotated around the dyad axis. The extension of the DNA ends resulted mostly from the rotation itself and from reorganization of already unwrapped DNA.

Phase IV: inner DNA turn opening

The DNA unwrapping process proceeded differently for the complete and tailless nucleosomes. For both structures, a second barrier for further unwrapping of DNA was apparent
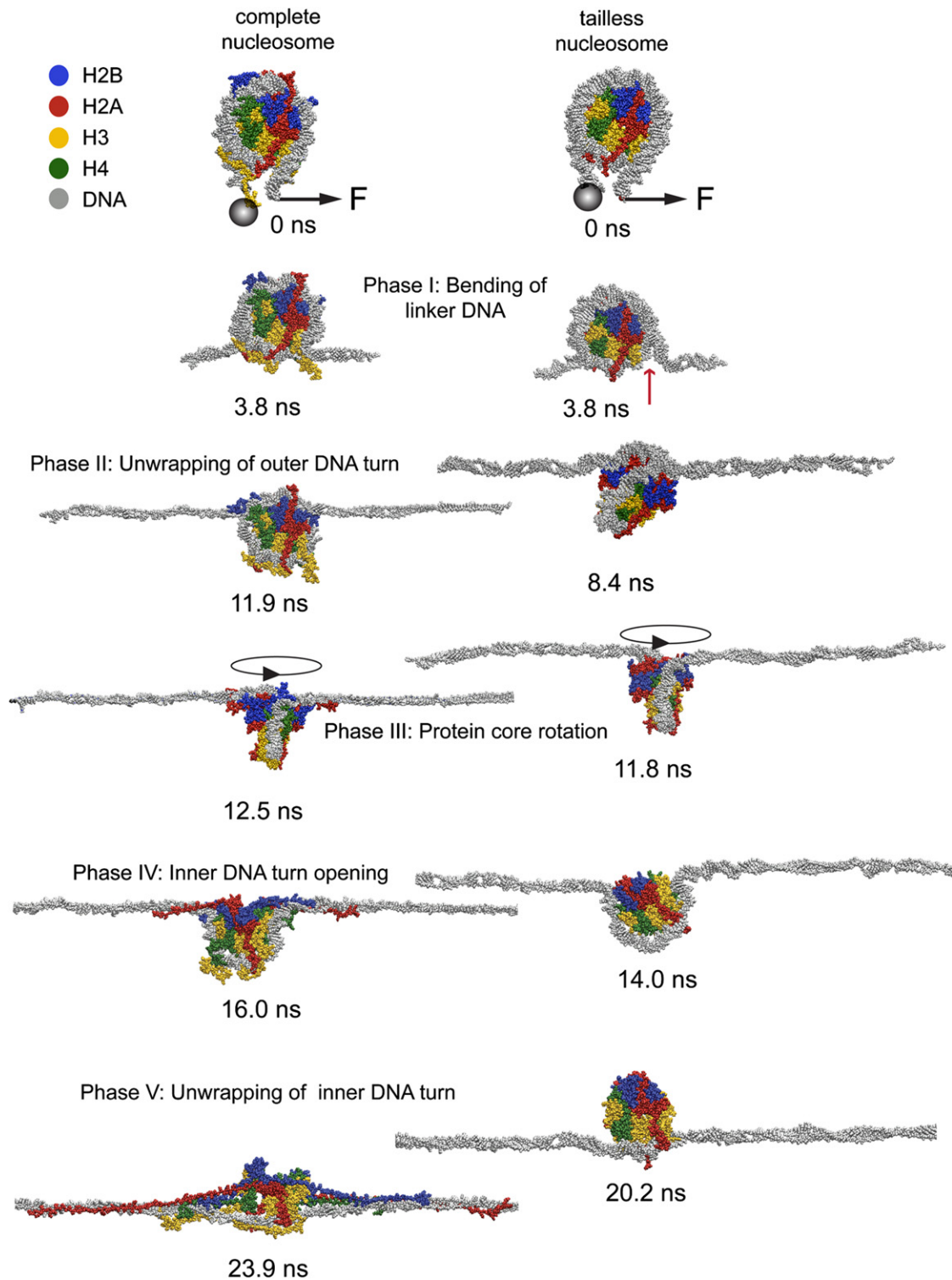
FIGURE 2 Intermediate structures formed during the DNA unwrapping process of a complete and a tailless nucleosome. The last nucleotide in the linker DNA on one side of the nucleosome was fixed (represented by the *gray sphere*), whereas the C1′ atom of the last nucleotide of the opposite linker DNA was moved along the indicated direction with an additional harmonic potential. Snapshots of the complete (*left panel*) and the tailless (*right panel*) nucleosomes at the indicated times of the SMD simulations are displayed. The complete trajectory is shown in Movie S2 and Movie S3. (Color code: H2B, *blue*; H2A, *red*; H3, *yellow*; H4, *green*; and DNA, *gray*.)
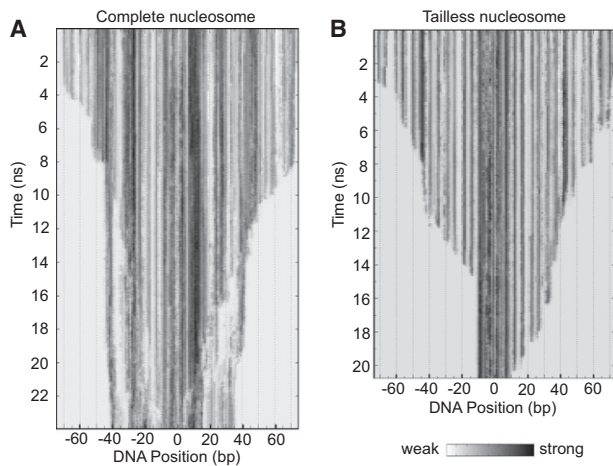
FIGURE 3 Temporal evolution of electrostatic and van der Waals interactions between DNA and histones during the unwrapping simulations. Changes of relative interaction strength from strong (*black*) to no-interaction (*white*) during the unwrapping simulations are shown. Contacts broke first between the histone protein residues and DNA bp closest to the DNA entry-exit site of the nucleosome. Regions with differences in disruption of interactions between complete and tailless nucleosomes were found around bp −18 to −25, −35 to −42, and 20 to 35 where the histone tails maintained contacts even with the completely unwrapped DNA. (*A*) Complete nucleosome. (*B*) Tailless NUCΔtail structure.

around bp position ±45. This was more pronounced for the NUC structure due to the DNA binding of H2A and H2B N-terminal tails. In addition, a partial disassembly of the histone core protein secondary structure occurred. It involved the disruption of interactions between the two H2A·H2B dimers due to changes of the relative location of α-helices in the histone fold and their partial unwinding. The latter process was apparent in both H2A histones in the first N-terminal α-helix (at ~62 nm/~75 nm extension, $t =$ ~13.4 ns/~16.1 ns) as well as in the second (at ~71 nm/ ~78 nm extension, $t =$ ~15.1 ns/~16.7 ns).

Both H2Bs displayed an opening of the angle between the two C-terminal α-helices at extension ~92/~113 nm and $t =$ ~19.5 ns/~21.5 ns. This was more pronounced for the H2B histone that rearranged first, which also showed a subsequent widening of the angle between the first N-terminal α-helices (extension ~96.5 nm, $t =$ ~21.4 ns). In addition, the H2A·H2B dimers were shifted slightly relative to the H3·H4 tetramer. The $(H3·H4)_2$ complex conformation itself was much less affected. Only in one H3 histone the first N-α-helix unwound (extension ~101 nm, $t =$ ~20.2 ns), whereas the other H3 and both H4s did not change their folding. For DNA unwrapping from the tailless nucleosome, no reorganization of the histone octamer structure was apparent. The opening of the inner DNA turn comprised the disruption of the DNA-core histone interactions at ±45 bp.

Phase V: unwrapping of inner DNA turn

DNA-core histone contacts were successively disrupted until the DNA was completely straightened along the direc-

tion of the applied force. Residual contacts between the globular histone domains and the stretched DNA remained only at the former dyad axis. In addition, some histone tail-DNA interactions persisted.

The N-terminal histone tails and the H2A C-terminal tail counteract DNA dissociation from the nucleosome

The H3 N-terminus and the H2A C-terminus contributed to the first barrier toward nucleosome unwrapping because they interacted with the DNA at the entry-exit site (see Fig. S4 and Fig. S7). Both tails were located in the minor groove and bind DNA via a variety of electrostatic and van der Waals interactions as well as hydrogen bonds. After linker DNA bending to ~90° relative to the nucleosomal DNA, the structure extended due to DNA stretching with partial DNA unstacking. Because the latter process is energetically unfavorable, the H3 and H2A tails must provide a significant contribution to the histone DNA interaction that prevented DNA unwrapping during a ~4-ns time period at the ±70 bp boundary (Fig. 3 *A*). At ±40 bp, the N-terminal H2A and H2B tails stabilized the inner DNA turn.

In response to the applied potential, the N-terminal α-helices of H2A started to break open after ~16 ns. This transition allowed it to maintain DNA contacts with the H2A and H2B tails (Fig. 2, Fig. 3 *A*, and Movie S2). Interestingly, the histone tails remained associated with the DNA during the entire 24-ns simulation period up to the point when the DNA was fully unwound from the histone octamer core. Their flexible conformation accommodated the significant DNA extension in the SMD experiments. The above contributions of the histone tails can be identified from the behavior of the NUCΔtail structure in the SMD simulations (Fig. 2, Fig. 3 *B*, and Movie S3), which displayed the following differences as compared to the complete nucleosome: 1), The first breakage of histone-DNA contacts at −70 bp occurred before 3.8 ns (Fig. 2, indicated by the *arrow*). 2), After breaking the contacts at ±70, the DNA dissociated more continuously from the protein core. 3), The second energy barrier toward unwrapping at ±40 bp was much less pronounced. 4), DNA-histone interactions remained only over a small region of ~20 bp in the unwrapped structure (Fig. 3 *B*).

Differences in the stability of the inner and outer DNA turn are partly due to additional histone tail-DNA interactions when the outer turn is unwrapped

In experimental studies, an apparent higher stability of the inner DNA turn has been reported (19,22,23,39). As proposed previously, this could include a contribution of the histone tails (39,40): While the tails are bound to both

DNA turns in a complete nucleosome, they might reposition to the inner turn as soon as the outer turn is unwrapped. We calculated the DNA interactions of all histone tails separately over the unwrapping trajectory. An ~20% fraction of histone tail interactions rearranged from the outer to the inner DNA turn during unwrapping of the outer DNA turn at ~12 ns, resulting in a moderate stabilization of the inner DNA turn (Fig. S8). The most relevant histone tail rearrangements involved in this process took place for the N-terminal tails of H2A, H2B, and H4. For example, after ~15 ns, the DNA interaction of the N-terminal tail of one histone H2A (*top-left image* in Fig. S8) increased as indicated by a change of the color coding to dark blue and relocated from a position at ~+42 bp toward +30 bp. In addition, both H2B N-termini displayed significant movements in the >12-ns time regime, and to a somewhat lesser extent the same was observed for the H4 tails.

In addition to changes of the histone tail location, the two DNA turns might repel each other while being wrapped around the histone proteins, and the inner turn might be stabilized by a reduced repulsion when the outer DNA turn is unwrapped (39,40). Our analysis of the DNA-DNA strand repulsion revealed a nonhomogeneous relatively low repulsion of 1–10% of the total calculated interaction energy at only a few bp positions (see Fig. S9). If averaged over the entire nucleosome, this value was reduced to a minor fraction of the total DNA-histone interaction energy. Accordingly, the effect of DNA repulsion on destabilizing the outer DNA turn appears to be negligible.

The force extension curve of unwrapping nucleosomal DNA results from a complex overlay of stretching and disruption events

Fig. 4 shows force-extension curves computed from the unwrapping simulations of the complete and tailless nucleosomes. Some of the most prominent peaks in the simulation trajectory of the NUC structure can be assigned to specific intermediates. The peaks at an extension of 20 nm, 37 nm, or 54 nm clearly originated from breaking DNA-histone contacts. The subsequent relaxation event at the 57–66 nm extension reflected the rotation of the protein core. The positive slope at 66–78 nm extension was due to the breaking of interactions between histone-dimers. The large force increase at extension ~85 nm resulted from numerous single disruption events that arose from a collapse of secondary structure interactions between two H2A histone and the N-terminal α-helices of one H2B histone. The final binding site opening event within the outer turn in the simulations correlated with the first disruption event observed experimentally (23) (see Fig. S10).

An unexpected contribution to the force extension curve was the persistence of histone tail contacts with the inner DNA turn throughout the stretching simulations. These induced a partial resolution of secondary structure and
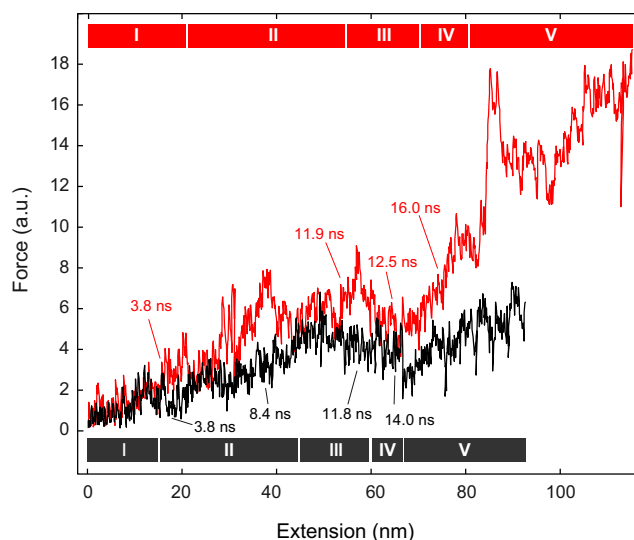

FIGURE 4 Virtual force spectroscopy of nucleosome unwrapping. From the SMD simulations, force spectroscopy curves were computed. The assignment of the five unwrapping phases and intermediates according to the indicated simulation times corresponds to that given in Fig. 2. The complete nucleosome structure (*red line*) is shown in comparison to the NUCΔtail structure (*black line*).

opening of the histone octamer complex. Because this process was overlaid with breaking of DNA-histone contacts, the identification of distinct intermediates of the unwrapping process becomes increasingly difficult (see Fig. S10). This contribution has, so far, not been considered in the interpretation of force spectroscopy experiments that do not provide sufficient resolution to dissect structural transformations on the nanometer lengthscale. In the virtual force spectroscopy curve of the NUCΔtail structure, the peaks that preceded the breakage of DNA-histone interactions were less pronounced. The unwrapping of the outer DNA turn occurred significantly faster, consistent with the lacking contributions from the H3 N-terminus and the H2A C-terminus. A corresponding effect was observed at the ±40 bp energy barrier that was largely reduced in the absence of histone tails.

DISCUSSION

The investigation of biologically relevant large-scale motions of the nucleosome is a challenging task because molecular dynamics simulations are currently limited to the nanosecond timescale (26,28,29). In contrast, experimental data suggest that processes such as nucleosome breathing, linker DNA opening, and sliding of nucleosomes occur spontaneously at the microsecond timescale and beyond (13,14). One approach to close this gap between experiments and theory is the use of coarse-grained models (33,41,42). However, these require some a priori knowledge of the system features to devise a description that preserves the characteristic properties to be studied. Alternatively, the

technique of steered molecular dynamics can be applied to direct motions via an externally applied force, so that the associated conformational rearrangements can be investigated within a time period that is accessible to MD simulations.

So far, SMD has been used primarily to visualize force-induced protein unfolding events of small systems with roughly 200 amino acids (29,43–45). Larger systems investigated with SMD approaches focused mostly on local structural changes by translocating a relatively small structure with respect to a bigger macromolecule (46–49). For example, in a study by Ishida and Hayward (49), a small peptide was pulled to move through the ribosome. It is noted that the magnitude and fluctuations of the forces applied in our constant-velocity SMD simulations depended on the parameters used for stretching velocity and spring constant. As discussed previously, a limitation of the SMD simulations is it that the currently available computational resources impose the use of stretching velocities that are orders-of-magnitude faster than those used in the experimentally conducted force spectroscopy experiments (29,36–38). Accordingly, it is expected that random structural fluctuations on a larger timescale than that observed here could largely facilitate the unwrapping process at lower stretching speed. Furthermore, force peak values larger than those recorded in experiments, and a loss of details on conformational changes that occur during the force-induced transitions, are to be expected. Nevertheless, the currently available cases of SMD simulations in comparison with experimental data demonstrate that valuable information can be obtained that was later validated in experimental studies (29).

Here, we applied a combination of MD and SMD to dissect the details of DNA-histone protein interactions, and to investigate the process of unwrapping the DNA from the histone octamer core. Our MD and SMD simulations revealed nucleosome dynamics for all-atom structures to identify the biologically relevant structural transitions at a resolution that cannot be reached in the experimental studies. The molecular dynamics of the nucleosome in an approximately physiological aqueous environment provided a DNA-histone interaction map at bp resolution (Fig. 1 A and see Fig. S2). From the analysis, a five-nucleotide periodicity pattern emerged that originated from contacts alternating between the two DNA strands of the double-helix. This is in agreement with conclusions from recent force spectroscopy experiments (22). Previously published histone-DNA interaction maps based on the crystal structure of the nucleosome (1,2) or on stretching experiments (22,23,50) identified a ~10-bp periodicity of interactions of the DNA with the histone proteins. These were assigned to 14 main interaction sites at regions where the minor groove faces inwards. Our MD analysis indicates that each of these interaction sites can be considered as comprising two ~5-bp separated contacts between each of the two individual DNA strands and the histone octamer.

The main origin of variations between different MD trajectories arose from the interactions of the histone tails with the DNA. Due to their flexibility they can bind to DNA in numerous conformations. This is reflected by the lack of defined structural information on their location in the available crystal structures. In addition, it is clear from the asymmetric and different location of the tails observed in our simulations that various positions are equally possible. At this point of time, we are unable to evaluate the effect of the conformational flexibility of the tails in the simulations in a systematic manner due to the high demands in computation time.

Despite these limitations, two important conclusions can be drawn from the MD simulations: Except for the relocation of the H2A C-terminus (see Fig. S4) the histone N-terminal tails are relatively stably attached to a certain region of the DNA in the 100-ns time regime. Furthermore, on this timescale, the degree of spontaneous disruption of DNA-histone interactions at the entry-exit site of the DNA in the nucleosome as well as at the start/end of the looped region in the NUC and NUC_loop structures was limited to 1–2 bp. This is in agreement with experimental studies, concluding that this almost completely wrapped state has a lifetime of several seconds that are interrupted by open periods of a few tenths of a second, in which up to 80 bp of nucleosomal DNA are spontaneously exposed (13–15). For this process, the energy barrier at ± 70 bp, which is stabilized by interactions of the H3 tail and the C-terminus of H2A, has to be broken.

The comparative SMD analysis conducted here revealed a large influence of the unstructured histone tails on the stability and mobility of nucleosomes (Figs. 2–4 and see Movie S2 and Movie S3). This is supported by previous MD simulations of nucleosome dynamics (28) and the MD simulations presented here. Our SMD analysis is in good agreement with force spectroscopy experiments (21). These show that the amount of outer-turn DNA wrapping was reduced by ~60% if the histone tails were removed. The primary contribution to this effect was from the H3 and H4 N-terminal tails. This agrees with our conclusion on the H3 tail interactions as opposing unwrapping of outer turn DNA. In addition, the removal of the H2A/H2B tails reduced histone-DNA interactions at $\sim \pm 36$ bp in the experiments, which is in line with our findings on the contribution of the H2A tail in the SMD simulations. In the cell, the H3 and H4 interactions are subject to regulation via acetylation or methylation of lysine residues.

In the in vitro experiments, the acetylation of histones H3 and H4 is clearly apparent in the experimental force spectroscopy curves as a factor that weakens histone-DNA interactions (21). Furthermore, numerous proteins recognize specifically modified histone tails as binding signals and would disrupt the tail-DNA interactions in their bound state. These include, for example, heterochromatin protein HP1 binding the H3 tail via its chromodomain (51), the

interactions of the PCAF, Brd2, Brd4, and BRDT bromodomains with acetylated H4 tails (52), and the binding of the H2A C-terminus to linker histone H1 (5). Our SMD studies revealed large contributions from the N-termini of H2A, H2B, H3, and H4 and the C-terminal histone H2A tail to DNA binding within the nucleosome. In particular, the N-terminus of H3 and the C-terminus of H2A counteracted the initiation of DNA unwrapping by stabilizing DNA interactions at positions ~ ± 70 bp (Figs. 2 and 3 A). Binding of these tails by the protein factors mentioned above would prevent their DNA association and could represent a mechanism to facilitate unwrapping of a certain nucleosome. The second barrier opposing unwrapping of nucleosomal DNA was mapped in our simulations to the ± 45 bp positions.

These two regions were identified also in experimental studies as sites of strong DNA-histone interactions (22,23). A direct comparison of the simulated force-extension curves with the data from Mihardja et al. (23) is shown in Fig. S10 and depicts two distinct transitions in both the simulated and experimental curves: The removal of the outer DNA turn is reflected as a reduction in the force increase. This state has been referred to as the "unwrapping event of the outer DNA turn" in the experimental analysis (23), and a good agreement between the two curves is apparent. A second significant decrease of force was observed in our analysis that was assigned to the "unwrapping event of the inner DNA turn" in the experiments (23). However, although this part of nucleosomal DNA dissociation occurred at about the same DNA extension in both the experiments and simulations, it did not represent a defined unwrapping transition in the simulations. The SMD trajectories revealed numerous local dissociation events, DNA bending, and conformational rearrangements that took place over a relatively large force regime as opposed to a sudden release of the outer DNA turn. In general, an unwrapping step might not be apparent in the experimental force-extension curves due to the complex superposition of several processes: 1), linker DNA bends into the direction of the applied force, 2), DNA stretches, 3), DNA-histone contacts open, 4), the histone octamer rotates, and 5), its secondary and tertiary structure partially disassembles. We conclude that the assignment of peaks to a single conformational transition in the experimental force-extension curve is fraught with difficulties. In contrast, the trajectory of the SMD simulations revealed all details of the unwrapping process. From the complex response of the nucleosome conformation to the applied force, we identified a sequence of five main phases of the unwrapping process that are depicted in Fig. 2: Phase 1), Bending of linker DNA. Phase 2), Unwrapping of the outer DNA turn. Phase 3), Protein core rotation. Phase 4), Inner turn opening with partial breakage of the octamer structure if histone tails are present. Phase 5), The unwrapping of the inner DNA turn. It is noted that within each of these five phases, the flexibility of both the DNA and histones is considerable so that these regimes partly overlap.

Our MD and SMD simulations elucidate how histone-DNA interactions determine access to the DNA sequence information. The results are relevant in the context of modeling competitive transcription factor binding and the conformational properties of the nucleosome chain. The energy potential of the DNA unwrapping process was described in a previous study by a spool (representing the histone octamer) from which the adhesive DNA tube was removed when tension was applied (39,40). This coarse-grained model explained several features of the unwrapping process, and was applied to improve force spectroscopy simulations of nucleosome chains (53). However, it lacks details on the shape of the nonhomogeneous histone-DNA potential along the nucleosome surface revealed here. In particular, a histone tail-dependent widening of the histone core during the unwrapping process has not been considered previously. This opening occurred mostly via conformational changes in the two H2A·H2B dimers, which is consistent with previous experimental findings. In these a hexasome particle was identified as an intermediate during nucleosome (dis)assembly that lacked one H2A·H2B dimer (54). Thus, the H2A·H2B dimers appear to be the least stable part of the nucleosome. Their conformational flexibility could make a significant contribution to the histone-DNA interaction dynamics.

In summary, the MD and SMD simulations conducted here identify several features of the mechanism by which DNA unwraps from the histone octamer core that need to be considered in coarse-grained descriptions of the nucleosome. This leads to integrative modeling approaches as for example applied in a recent study on the competitive binding of transcription factors to nucleosomal DNA (11). Furthermore, it is anticipated that SMD simulations of the nucleosome along the lines described here will provide insights into the molecular mechanisms by which chromatin remodeling complexes translocate nucleosomes along the DNA.

SUPPORTING MATERIAL

REFERENCES

1. Luger, K., A. W. Mäder, …, T. J. Richmond. 1997. Crystal structure of the nucleosome core particle at 2.8 Å resolution. *Nature.* 389:251–260.

2. Davey, C. A., D. F. Sargent, …, T. J. Richmond. 2002. Solvent mediated interactions in the structure of the nucleosome core particle at 1.9 Å resolution. *J. Mol. Biol.* 319:1097–1113.

3. Polach, K. J., P. T. Lowary, and J. Widom. 2000. Effects of core histone tail domains on the equilibrium constants for dynamic DNA site accessibility in nucleosomes. *J. Mol. Biol.* 298:211–223.

4. Vitolo, J. M., C. Thiriet, and J. J. Hayes. 2000. The H3-H4 N-terminal tail domains are the primary mediators of transcription factor IIIA access to 5S DNA within a nucleosome. *Mol. Cell. Biol.* 20:2167–2175.

5. Vogler, C., C. Huber, …, R. Schneider. 2010. Histone H2A C-terminus regulates chromatin dynamics, remodeling, and histone H1 binding. *PLoS Genet.* 6:e1001234.

6. Campos, E. I., and D. Reinberg. 2009. Histones: annotating chromatin. *Annu. Rev. Genet.* 43:559–599.

7. Lee, B. M., and L. C. Mahadevan. 2009. Stability of histone modifications across mammalian genomes: implications for 'epigenetic' marking. *J. Cell. Biochem.* 108:22–34.

8. Wang, X., and J. J. Hayes. 2006. Physical methods used to study core histone tail structures and interactions in solution. *Biochem. Cell Biol.* 84:578–588.

9. Anderson, J. D., and J. Widom. 2000. Sequence and position-dependence of the equilibrium accessibility of nucleosomal DNA target sites. *J. Mol. Biol.* 296:979–987.

10. Hodges, C., L. Bintu, …, C. Bustamante. 2009. Nucleosomal fluctuations govern the transcription dynamics of RNA polymerase II. *Science.* 325:626–628.

11. Teif, V. B., R. Ettig, and K. Rippe. 2010. A lattice model for transcription factor access to nucleosomal DNA. *Biophys. J.* 99:2597–2607.

12. Park, Y. J., P. N. Dyer, …, K. Luger. 2004. A new fluorescence resonance energy transfer approach demonstrates that the histone variant H2AZ stabilizes the histone octamer within the nucleosome. *J. Biol. Chem.* 279:24274–24282.

13. Li, G., M. Levitus, …, J. Widom. 2005. Rapid spontaneous accessibility of nucleosomal DNA. *Nat. Struct. Mol. Biol.* 12:46–53.

14. Tomschik, M., H. Zheng, …, S. H. Leuba. 2005. Fast, long-range, reversible conformational fluctuations in nucleosomes revealed by single-pair fluorescence resonance energy transfer. *Proc. Natl. Acad. Sci. USA.* 102:3278–3283.

15. Koopmans, W. J., R. Buning, …, J. van Noort. 2009. spFRET using alternating excitation and FCS reveals progressive DNA unwrapping in nucleosomes. *Biophys. J.* 97:195–204.

16. Strohner, R., M. Wachsmuth, …, G. Längst. 2005. A 'loop recapture' mechanism for ACF-dependent nucleosome remodeling. *Nat. Struct. Mol. Biol.* 12:683–690.

17. Bowman, G. D. 2010. Mechanisms of ATP-dependent nucleosome sliding. *Curr. Opin. Struct. Biol.* 20:73–81.

18. Bennink, M. L., S. H. Leuba, …, J. Greve. 2001. Unfolding individual nucleosomes by stretching single chromatin fibers with optical tweezers. *Nat. Struct. Biol.* 8:606–610.

19. Brower-Toland, B. D., C. L. Smith, …, M. D. Wang. 2002. Mechanical disruption of individual nucleosomes reveals a reversible multistage release of DNA. *Proc. Natl. Acad. Sci. USA.* 99:1960–1965.

20. Pope, L. H., M. L. Bennink, …, J. F. Marko. 2005. Single chromatin fiber stretching reveals physically distinct populations of disassembly events. *Biophys. J.* 88:3572–3583.

21. Brower-Toland, B., D. A. Wacker, …, M. D. Wang. 2005. Specific contributions of histone tails and their acetylation to the mechanical stability of nucleosomes. *J. Mol. Biol.* 346:135–146.

22. Hall, M. A., A. Shundrovsky, …, M. D. Wang. 2009. High-resolution dynamic mapping of histone-DNA interactions in a nucleosome. *Nat. Struct. Mol. Biol.* 16:124–129.

23. Mihardja, S., A. J. Spakowitz, …, C. Bustamante. 2006. Effect of force on mononucleosomal dynamics. *Proc. Natl. Acad. Sci. USA.* 103:15871–15876.

24. Bishop, T. C. 2005. Molecular dynamics simulations of a nucleosome and free DNA. *J. Biomol. Struct. Dyn.* 22:673–686.

25. Korolev, N., and L. Nordenskiöld. 2007. H4 histone tail mediated DNA-DNA interaction and effects on DNA structure, flexibility, and counterion binding: a molecular dynamics study. *Biopolymers.* 86:409–423.

26. Bishop, T. C. 2008. Geometry of the nucleosomal DNA superhelix. *Biophys. J.* 95:1007–1017.

27. Ruscio, J. Z., and A. Onufriev. 2006. A computational study of nucleosomal DNA flexibility. *Biophys. J.* 91:4121–4132.

28. Roccatano, D., A. Barthel, and M. Zacharias. 2007. Structural flexibility of the nucleosome core particle at atomic resolution studied by molecular dynamics simulation. *Biopolymers.* 85:407–421.

29. Sotomayor, M., and K. Schulten. 2007. Single-molecule experiments in vitro and in silico. *Science.* 316:1144–1148.

30. Li, P.-C., and D. E. Makarov. 2004. Simulation of the mechanical unfolding of ubiquitin: probing different unfolding reaction coordinates by changing the pulling geometry. *J. Chem. Phys.* 121:4826–4832.

31. Gräter, F., J. Shen, …, H. Grubmüller. 2005. Mechanically induced titin kinase activation studied by force-probe molecular dynamics simulations. *Biophys. J.* 88:790–804.

32. Schalch, T., S. Duda, …, T. J. Richmond. 2005. X-ray structure of a tetranucleosome and its implications for the chromatin fiber. *Nature.* 436:138–141.

33. Voltz, K., J. Trylska, …, J. Smith. 2008. Coarse-grained force field for the nucleosome from self-consistent multiscaling. *J. Comput. Chem.* 29:1429–1439.

34. Phillips, J. C., R. Braun, …, K. Schulten. 2005. Scalable molecular dynamics with NAMD. *J. Comput. Chem.* 26:1781–1802.

35. Case, D. A., T. A. Darden, …, P. A. Kollman. 2008. AMBER 10. University of California, San Francisco, CA.

36. Harris, S. 2003. The physics of DNA stretching. *Contemp. Phys.* 45:11–30.

37. Balsera, M., S. Stepaniants, …, K. Schulten. 1997. Reconstructing potential energy functions from simulated force-induced unbinding processes. *Biophys. J.* 73:1281–1287.

38. Gullingsrud, J., R. Braun, and K. Schulten. 1999. Reconstructing potentials of mean force through time series analysis of steered molecular dynamics simulations. *J. Comput. Phys.* 151:190–211.

39. Kulić, I. M., and H. Schiessel. 2004. DNA spools under tension. *Phys. Rev. Lett.* 92:228101.

40. Kulic, I. M., and H. Schiessel. 2008. Opening and closing DNA: theories on the nucleosome. *In* DNA Interactions with Polymers and Surfactants. R. S. Dias and B. Lindman, editors. Wiley, London, UK. 173–208.

41. Sharma, S., F. Ding, and N. V. Dokholyan. 2007. Multiscale modeling of nucleosome dynamics. *Biophys. J.* 92:1457–1470.

42. Arya, G., and T. Schlick. 2006. Role of histone tails in chromatin folding revealed by a mesoscopic oligonucleosome model. *Proc. Natl. Acad. Sci. USA.* 103:16236–16241.

43. Krammer, A., H. Lu, …, V. Vogel. 1999. Forced unfolding of the fibronectin type III module reveals a tensile molecular recognition switch. *Proc. Natl. Acad. Sci. USA.* 96:1351–1356.

44. Genchev, G. Z., M. Källberg, …, H. Lu. 2009. Mechanical signaling on the single protein level studied using steered molecular dynamics. *Cell Biochem. Biophys.* 55:141–152.

45. Gao, M., D. Craig, …, K. Schulten. 2002. Identifying unfolding intermediates of FN-III(10) by steered molecular dynamics. *J. Mol. Biol.* 323:939–950.

46. Cuendet, M. A., and O. Michielin. 2008. Protein-protein interaction investigated by steered molecular dynamics: the TCR-pMHC complex. *Biophys. J.* 95:3575–3590.

47. Grubmüller, H., B. Heymann, and P. Tavan. 1996. Ligand binding: molecular mechanics calculation of the streptavidin-biotin rupture force. *Science.* 271:997–999.

48. Lüdemann, S. K., V. Lounnas, and R. C. Wade. 2000. How do substrates enter and products exit the buried active site of cytochrome P450cam? 2. Steered molecular dynamics and adiabatic mapping of substrate pathways. *J. Mol. Biol.* 303:813–830.

49. Ishida, H., and S. Hayward. 2008. Path of nascent polypeptide in exit tunnel revealed by molecular dynamics simulation of ribosome. *Biophys. J.* 95:5962–5973.

50. Brower-Toland, B., and M. D. Wang. 2004. Use of optical trapping techniques to study single-nucleosome dynamics. *Methods Enzymol.* 376:62–72.

51. Maison, C., and G. Almouzni. 2004. HP1 and the dynamics of hetero-chromatin maintenance. *Nat. Rev. Mol. Cell Biol.* 5:296–304.

52. Zeng, L., and M. M. Zhou. 2002. Bromodomain: an acetyl-lysine binding domain. *FEBS Lett.* 513:124–128.

53. Kepper, N., R. Ettig, …, K. Rippe. 2011. Force spectroscopy of chromatin fibers: extracting energetics and structural information from Monte Carlo simulations. *Biopolymers.* 95:435–447.

54. Mazurkiewicz, J., J. F. Kepert, and K. Rippe. 2006. On the mechanism of nucleosome assembly by histone chaperone NAP1. *J. Biol. Chem.* 281:16462–16472.

Supporting Information

Dissecting DNA-histone interactions in the nucleosome by molecular dynamics simulations of DNA unwrapping

Ramona Ettig, Nick Kepper, Rene Stehr, Gero Wedemann and Karsten Rippe

Supplementary Methods

All-atom nucleosome structures

Simulations of the complete (NUC) and tailless (NUCΔtail) nucleosome were based on the start structure of nucleosome and linker DNA from the tetranucleosome crystal structure 1zbb (1) that had undergone minimization and had been solvated and equilibrated for 50 ns (2) (Fig. S1 A). A second MD simulation was conducted with a nucleosome start structure derived from the same crystal structure, which was minimized and equilibrated for ~2 ns. For simulations of the NUCΔtail structure the N-terminal tails were removed from the 50-ns equilibrated complete nucleosome structure so that only amino acids 41-135 (H3), 25-102 (H4), 17-128 (H2A), and 32-122 (H2B) remained. The NUC_loop structure with a central DNA loop was created from NUC by shifting a DNA fragment containing base pairs 66 to 139 by ~3.4 nm and adding 10 additional base pairs on both sides to connect it again with the rest of the nucleosomal DNA (Fig. S1 B). Thus, the total length of the nucleosomal DNA was increased by 20 base pairs to 167 bp and the total DNA length included in the simulations was 184 base pairs. The DNA transition joints were aligned and connected. Subsequently, several rounds of minimization for 50 000 steps were conducted with decreasing constraints around 10 base pairs of each of the new DNA connections in vacuum. In addition, the nucleosome crystal structure NUC_A_{16} with an adenine $dA_{16} \cdot dT_{16}$ insert (pdb 2fj7) (3) was used for analysis.

Preparations for the simulations were done with Amber 10.0 (4): The nucleosome structure (complete or without tails) was placed in a ~22 x 20 x 14.8 nm^3 box of TIP3P water molecules (5). It contained 262 Na^+ ions to neutralize the DNA phosphate charges and an additional 950 Na^+ and Cl^- ions, which provided a salt concentration of 150 mM. The ions and water molecules were placed using the Amber 10.0 *xleap* module. The minimum distance to the water box borders was 15 Å for the MD simulations. The NUC_loop structure was neutralized with 218 Na+ ions and placed in a water box of 3 121 nm^3 volume (20.5 x 14.5 x 10.5 nm^3) including 270 Na^+ and 270 Cl^- ions to yield a salt concentration of 150 mM. The solvated structure was again minimized with constraints on all parts that had not been changed, so that initially only the newly generated DNA loop could adjust in the solution.

All simulation starting structures were minimized for 10 000 steps with slowly released constraints on all nucleosome atoms with the *sander* module of the Amber 10.0, using the *parm99* force field (6). The positional constraints were established with an additional harmonic potential $\sim k\Delta x$ added to each specified atom and decreased successively every 1 000 steps with k = 100, 10, 5, 2, 1, 0.1, 0.01 and 0 kcal mol^{-1} Å^{-2}. The solvent was heated in 25 000 steps from 0 to 300 °K. The volume adjusted in an environment with constant pressure and constant temperature (NPT ensemble) for 150 000 steps and an additional 50 000 steps were calculated in an environment with constant volume and constant energy (NVE ensemble) to check energy conditions and stability. The final systems were equilibrated for 2 ns resulting in the NUC and NUC_loop start structures shown in Fig. S1 and in that of the nucleosome without tails (not shown). References to specific DNA sites relative to the histone octamer are marked according to their super helix location (SHL).

MD and SMD simulations

For MD and SMD simulations of minimized and equilibrated nucleosome structures the NAMD 2.6 software package (7) was used on the "ICE1 and XE Clusters" of the supercomputer facility 'North-German Supercomputing Alliance, HLRN'. The nodes were equipped with Intel Xeon Harpertown E5472 processors operating at 3.0 GHz with two sockets per node, four cores per socket and 8 cores per node. In the simulations 256 to 1024 cores were used. Parallelization was most efficient for 512 cores with a 1-2 ns simulation trajectory (depending on the size of the system) in 12 hours runs.

MD simulations of the nucleosome structures were conducted in an NPT environment in explicit water for ~20 ns, with periodic boundary conditions. The RATTLE algorithm (8), Langevin Temperature control (T = 300 °K), constant pressure control (Langevin Piston (9), at 1.01 bar pressure) and force cutoff of 12 Å were applied, and the electrostatic interactions were treated with the particle mesh Ewald option (10).

The SMD simulations were calculated in NVE ensemble with constant boundary conditions, applied RATTLE algorithm, and a force cutoff of 12 Å. Both NUC and NUCΔtail were stretched with v_c = 0.05 Å ps^{-1} and spring constant k = 2 kcal mol^{-1} Å^{-2}. To completely unwrap the DNA from the nucleosome core one end of the nucleosomal linker DNA was fixed (i.e. residue +83) and a harmonic spring potential at atom C1' of residue -83 at the opposite linker of the nucleosome was applied. Thus, the stretching forces affected primarily one strand of the DNA double helix, and the second strand could rotate freely around the first strand to relax torsion stress. The SMD simulations were conducted with both the complete and the tailless nucleosome structures. The 17 x 30 x 10.5 nm^3 water boxes were aligned in xyz-coordinates, and the +y-axis was chosen as force direction. Due to the large size of the system the NAMD protocol for constant velocity SMD was used. During the simulations the

water box had to be enlarged twice to dimensions of 12 x 47 x 11 nm^3 and 17.6 x 81.5 x 12 nm^3, respectively, to account for the extension of the structure. Ions were transferred from the previous box into the new one and additional water molecules and ions were added. Then water and ion heating and equilibration were conducted for ~150 000 steps while the structure atoms were constrained. Subsequently, the simulations were continued as described above.

The analysis of interaction strength was performed with the NAMD energy plugin of VMD (version 1.8.6) that was also used to visualize trajectories and structures (11). For every 20 ps of MD trajectories electrostatic and van der Waals interactions were calculated. These were computed between one nucleotide of each DNA strand and the entire histone octamer for complete interaction maps, or only with the histone residues of its globular parts. To analyze the periodicity, the Fourier spectra of the time-averaged values were calculated with the MATLAB software.

The webpage http://www.EpiGenSysMO.org provides MD trajectories in PDB format of the MD and SMD simulations used in this publication with 20 ps time resolution. The files can be accessed after registration. All simulations were done with water boxes and ions, but to reduce file size the condensed trajectories lack water and ions. Two MD simulation trajectories of nucleosomes for 20 ns simulation time are available and one MD simulation for 120 ns of the NUC_loop structure (each consisting of 10 or 64 single simulation trajectories, respectively, see also Movie S1). For the SMD simulations of nucleosome unwrapping the NUC and the NUCΔtail structures shown in Fig. 2 and 3 and in the Movies S2 and S3 have been deposited. These comprise 24 ns (NUC) and 20 ns (NUCΔtail) and consist of up to 30 single simulation trajectories that have been combined into each one pdb file.

Supplementary Results

MD simulations of the equilibrated NUC_loop structure in explicit water were conducted for a total time of 120 ns in 64 single simulations each on 512 cores for 12 h running times, respectively, i. e. the total computation time was ~33 days. During the MD simulations the artificially induced DNA loop remained in a relatively stable conformation (Fig. S5, Fig. S6, Movie S1). The magnitude of conformational fluctuations was comparable to that of the linker DNA. DNA translocations were analyzed by evaluating three superhelix locations (SHLs) in the loop referred to as SHLx$_1$, SHLx$_2$ and SHL -3.5 (Fig. S6 A). The temporal evolution of the distances of these positions to the center of the histone octamer is shown in Fig. S6 B. The maximal displacement during the 120 ns for all three positions was ~10 Å. Although loop position SHL -3.5 and SHLx$_1$ were separated by only ~20 base pairs their movements appeared to be mostly independent. In contrast, neighboring SHLs of DNA

attached to the histone octamer in other parts of the nucleosome structure displayed highly correlated distance changes to the center at this DNA separation length. During the simulations the initially smoothly bent DNA in the loop became somewhat kinked in the central region (Fig. 6C). In Figure S6 D the temporal evolution of the radial distance to the center of mass of the system for the last (SHL -3.5) and first (SHL -2.5) interaction site of the loop is plotted in comparison to position SHL 3.5 within the inner DNA turn. Both the SHL -3.5 and -2.5 positions moved significantly more in radial direction than the SHL 3.5 reference. This radial motion described an opening or closing of the corresponding interaction sites in the loop. During the first 60 ns, SHL -3.5 moved closer to the histone octamer core (Movie S1, Fig. S5 and Fig. S6 D). After 60 ns the DNA started to slowly increase its distance again, resulting in an about 10 Å "breathing"-like motion during ~100 ns. Distance variations of position SHL -2.5 were significantly smaller but still exceeded that of the SHL 3.5 reference location. Both at the entry-exit site of the DNA at the nucleosome as well as at the start and end position of the loop, the transient opening/closing of DNA-histone interactions in the NUC_loop structure was restricted to 1-2 bp on the 100 ns time scale of the simulation.

Supplementary References

1. Schalch, T., S. Duda, D. F. Sargent, and T. J. Richmond. 2005. X-ray structure of a tetranucleosome and its implications for the chromatin fibre. Nature 436:138-141.

2. Voltz, K., J. Trylska, V. Tozzini, V. Kurkal-Siebert, J. Langowski, and J. Smith. 2008. Coarse-grained force field for the nucleosome from self-consistent multiscaling. J Comput Chem 29:1429-1439.

3. Bao, Y., C. L. White, and K. Luger. 2006. Nucleosome Core Particles Containing a Poly(dA.dT) Sequence Element Exhibit a Locally Distorted DNA Structure. 361:617-626.

4. Case, D. A., T. A. Darden, I. T. E. Cheatham, C. L. Simmerling, J. Wang, R. E. Duke, R. Luo, M. Crowley, R. C. Walker, W. Zhang, K. M. Merz, B. Wang, S. Hayik, A. Roitberg, G. Seabra, I. Kolossváry, K. F.Wong, F. Paesani, J. Vanicek, X. Wu, S. R. Brozell, T. Steinbrecher, H. Gohlke, L. Yang, C. Tan, J. Mongan, V. Hornak, G. Cui, D. H. Mathews, M. G. Seetin, C. Sagui, V. Babin, and P. A. Kollman. 2008. AMBER 10. University of California, San Francisco.

5. Jorgensen, W., J. Chandrasekhar, and J. Madura. 1983. Comparison of simple potential functions for simulating liquid water. J. Chem. Phys. 79:926-935.

6. Duan, Y., C. Wu, S. Chowdhury, M. C. Lee, G. Xiong, W. Zhang, R. Yang, P. Cieplak, R. Luo, T. Lee, J. Caldwell, J. Wang, and P. Kollman. 2003. A point-charge

force field for molecular mechanics simulations of proteins based on condensed-phase quantum mechanical calculations. J Comput Chem 24:1999-2012.

7. Phillips, J. C., R. Braun, W. Wang, J. Gumbart, E. Tajkhorshid, E. Villa, C. Chipot, R. D. Skeel, L. Kale, and K. Schulten. 2005. Scalable molecular dynamics with NAMD. J Comput Chem 26:1781-1802.

8. Miyamoto, S., and P. A. Kollman. 1992. SETTLE: An Analytical Version of the SHAKE and RATTLE Algorithm for Rigid Water Models. J Comput Chem 13:952-962.

9. Feller, S., Y. Zhang, and R. W. Pastor. 1995. Constant pressure molecular dynamics simulation: The Langevin piston method. J Chem Phys 103:4613-4621.

10. Darden, T., D. York, and L. Pedersen. 1993. Particle mesh Ewald - An N.Log(N) method for Ewald sums in large systems. J Chem Phys 98:10089–10092.

11. Humphrey, W., A. Dalke, and K. Schulten. 1996. VMD: visual molecular dynamics. J Mol Graph 14:33-38, 27-38.

12. Mihardja, S., A. J. Spakowitz, Y. Zhang, and C. Bustamante. 2006. Effect of force on mononucleosomal dynamics. Proc Natl Acad Sci USA 103:15871-15876.

Supplementary Figures
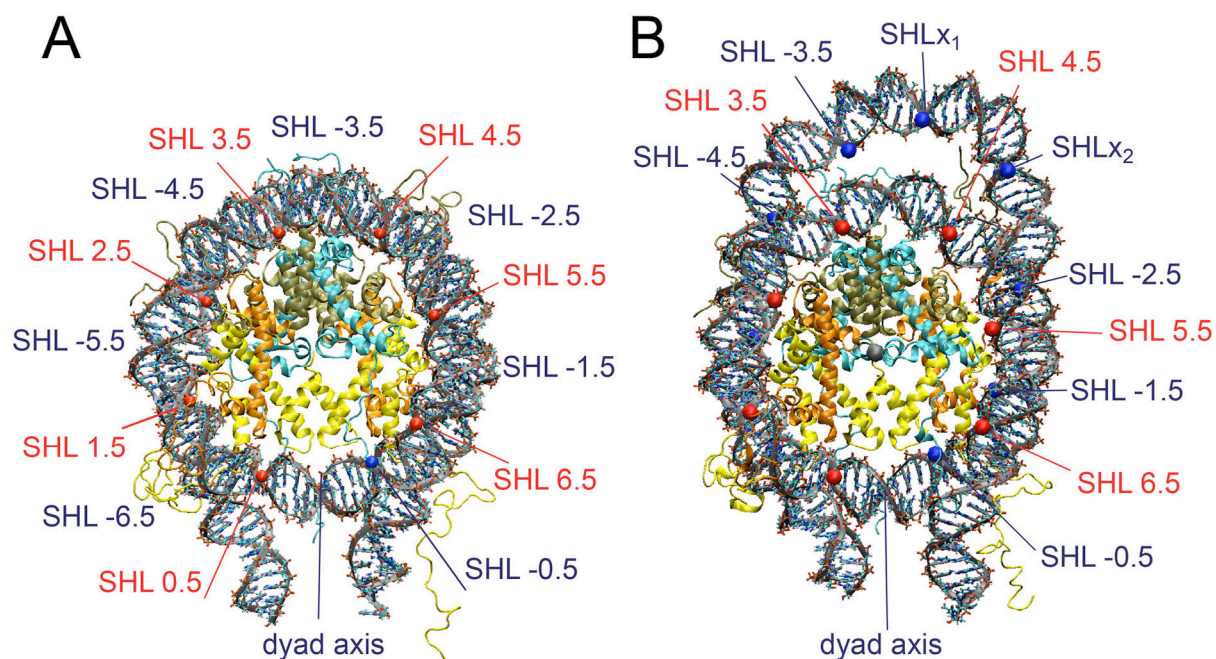
Figure S1. Nucleosome structures

Equilibrated nucleosome structures with indicated superhelix locations (SHLs). The numbering starts on the dyad axis of the nucleosome and follows the positions of the major groove of the nucleosomal DNA facing inwards to the protein. The red spheres indicate the positive positions, while the blue ones depict the negative SHLs in the back DNA turn. (A) Canonical nucleosome core particle in the NUC structure. (B) NUC_loop structure with an inserted DNA loop. With the loop two new SHL sites were introduced that are referred to as $SHLx_1$ and $SHLx_2$.
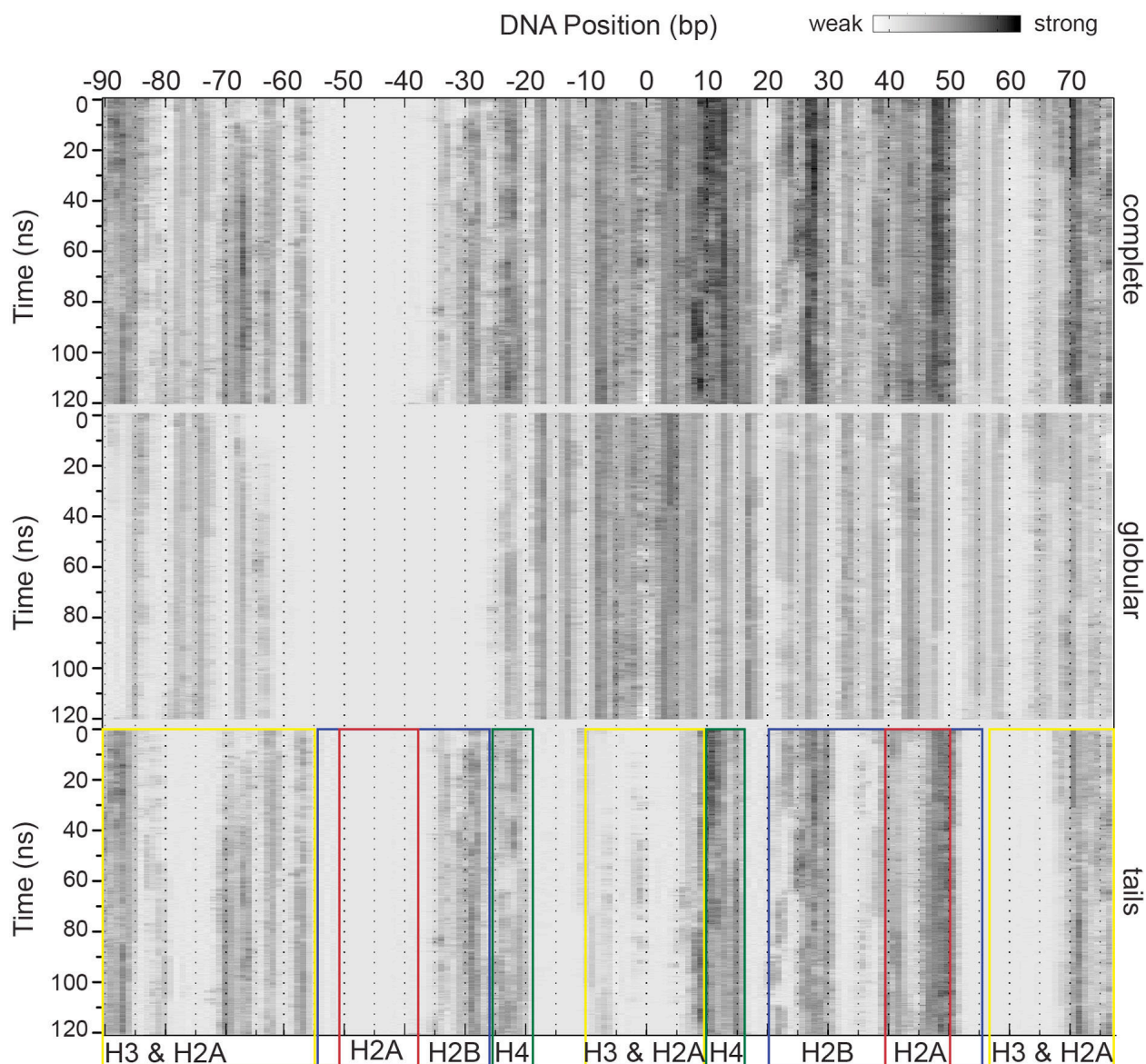
Figure S2. Temporal evolution of the histone-DNA interactions in the NUC_loop structure

The electrostatic and van der Waals interactions in the nucleosome with an additionally introduced loop were calculated for a 120 ns MD simulation trajectory. Interaction strength increases from white to black. The DNA position numbering refers to the central base pair 0 at the nucleosome dyad axis. The three panels differ with respect to the histone residues that were taken into account for calculating interaction energies with the DNA. They show the complete nucleosome ("complete", top panel), the interactions without the N-terminal tails ("globular", middle panel) and the isolated tail contributions ("tails", bottom panel). The colored boxes assign interactions to specific histone tails: H3 and H2A, yellow; H2A, red; H2B, blue; H4, green.
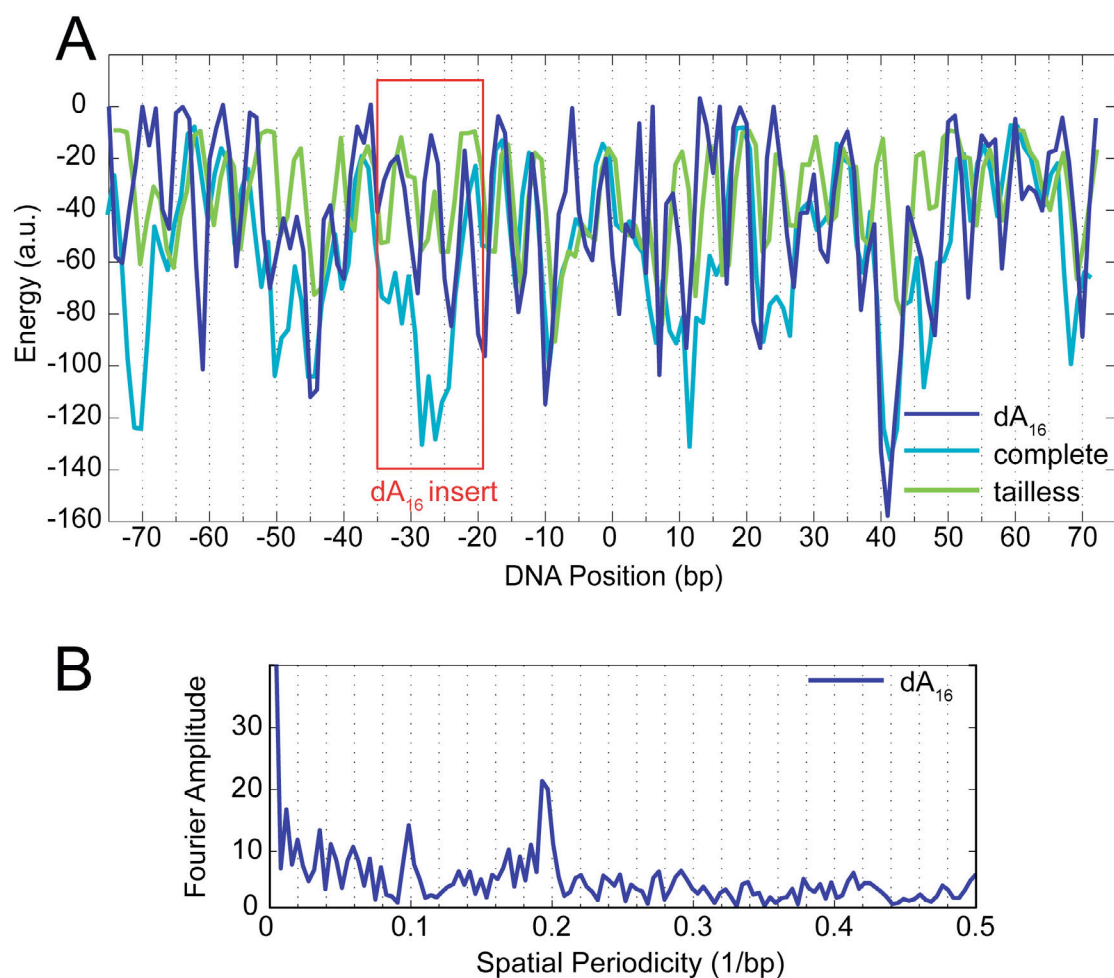
Figure S3. Histone-DNA interaction map for a nucleosome with d(A)$_{16}$ insert
(A) The DNA-histone interaction pattern of the NUC_A$_{16}$ nucleosome with a dA$_{16}$·dT$_{16}$ insert (pdb ID: 2FJ7) is shown in dark blue together with the NUC (cyan) and NUCΔtail (green) structures. (B) The Fourier analysis of NUC_A$_{16}$ revealed a dominant frequency at 0.19 /bp, i. e. a 5-nucleotide periodicity and a peak at 0.1/bp or 10 bp spatial distance.

H2A 1-114, 115-122, 123-129
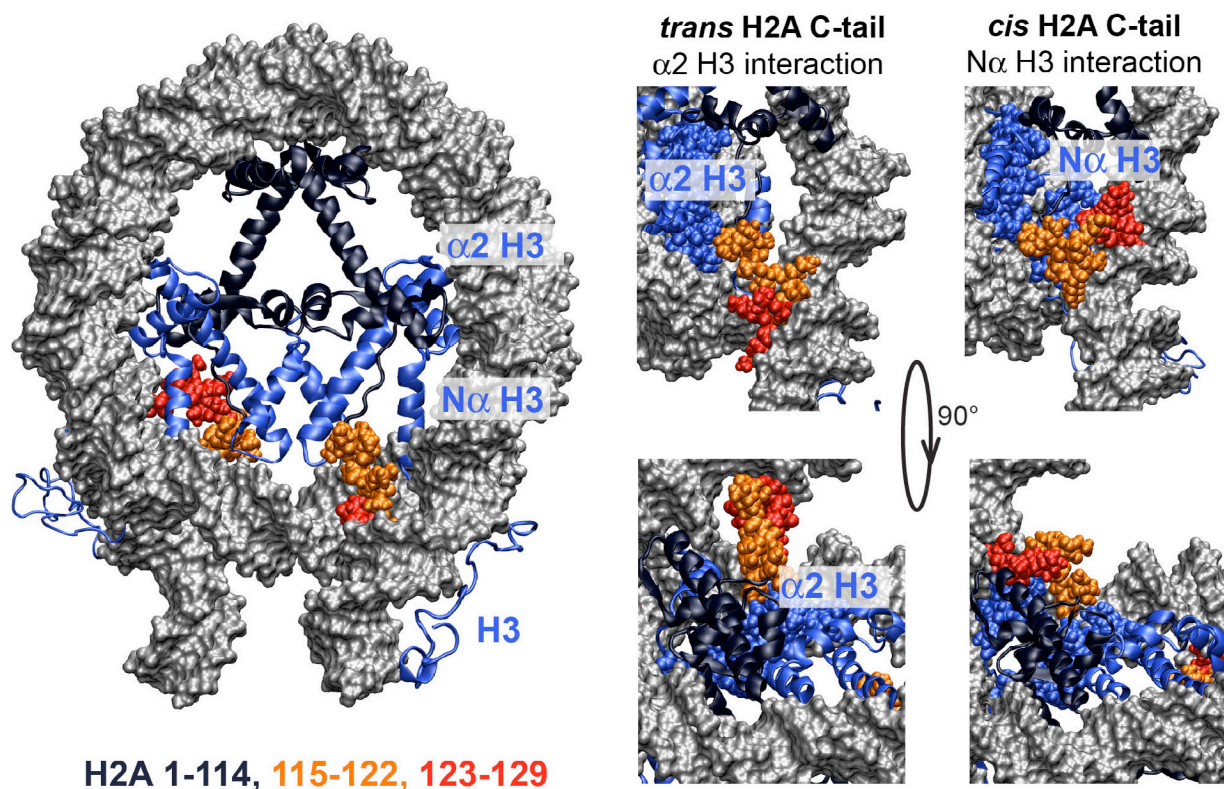
Figure S4. Dynamics of the H2A C-terminus during MD simulations

Histones H2A (black, red and orange) and H3 (blue) and DNA (gray) in the nucleosome complex are depicted. In the *trans* conformation the H2A C-tail is interacting with the minor groove of the linker DNA and with the α2 helix of H3. In the *cis* conformation additional interactions with the Nα H3 helix are made and interactions with the linker DNA occur with other base pairs. A conformation change between the *trans* and *cis* conformations of the H2A C-tail was the only major histone tail translocation observed on the ~100 ns time scale of the MD simulations.
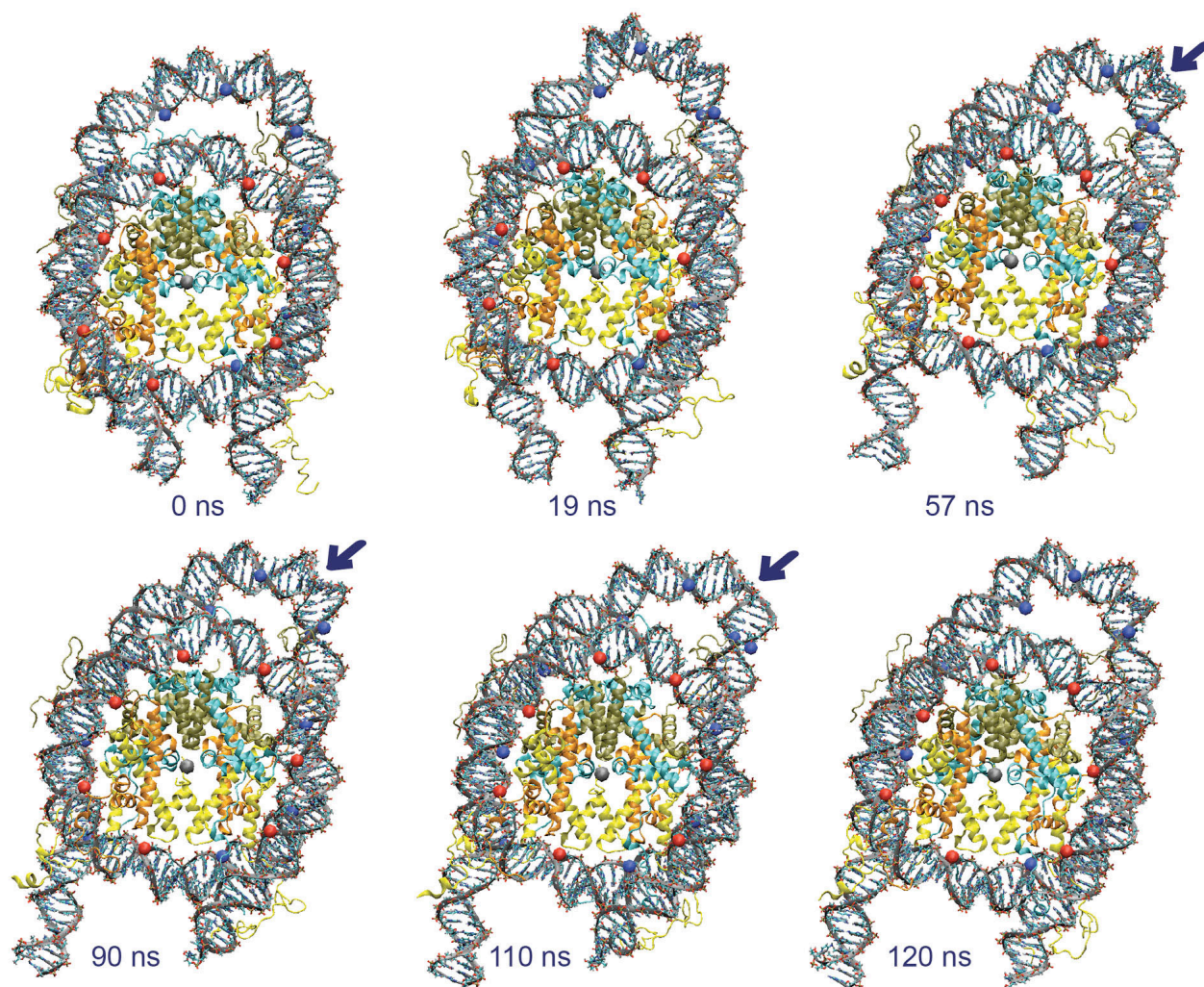
Figure S5. Time series of MD simulations of the NUC_loop structure

In comparison with the equilibrated and solvated system at 0 ns it can be seen that both the DNA loop as well as the linker DNA are moving due to thermal fluctuations. Arrows indicate changes in the loop geometry and the appearance of a DNA kink.
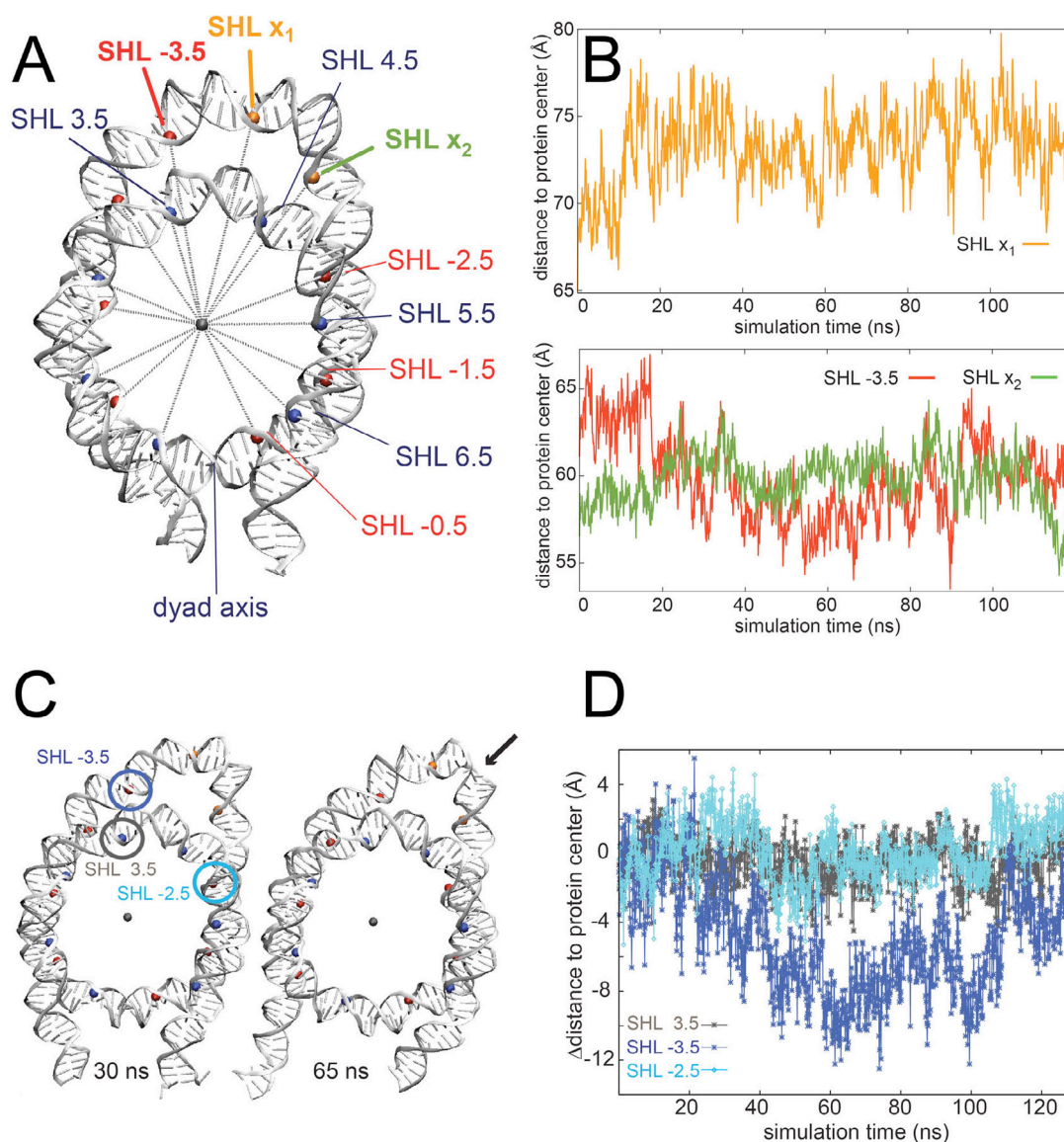
Figure S6. DNA loop dynamics in the NUC_loop nucleosome structure

(A) The DNA motions in the loop during the MD simulations were measured as the distances (gray lines) between the SHLs (colored spheres) to the center of the histone octamer protein core (gray sphere). (B) Displacement of sites SHL-3.5, $SHLx_1$ and $SHLx_2$ during the simulations. The translocations showed little correlations. (C) Snapshots of the NUC_loop structure. After 30 ns a strongly bent region between $SHLx_1$ and $SHLx_2$ had formed, which persisted for ~60 ns. (D) Distance of indicated SHL positions to the protein center. SHL -2.5 and SHL -3.5 mark the entry/exit regions of the DNA loop. As a reference point SHL 2.5 in the DNA turn that has no loop.
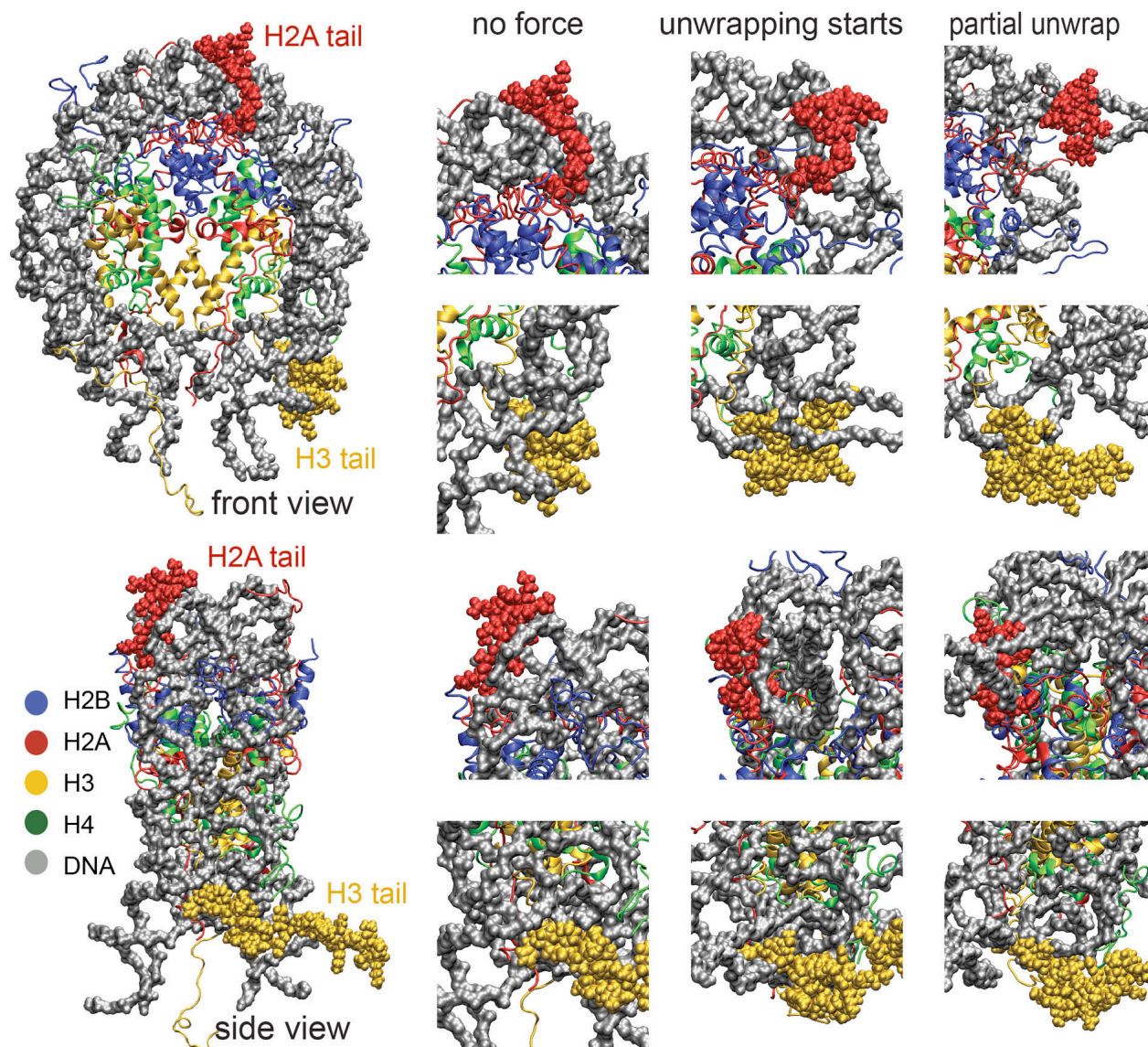
Figure S7. Dynamics of the H2A and H3 N-terminal tails during the SMD simulations of nucleosome unwrapping

The top panel depicts the front view of the H2A N-terminus (upper lane) and H3 tail (lower lane). The bottom panel is a side view of the H2A N-terminus (upper lane) and the H3 tail (bottom lane). The zoomed images show the conformation at the beginning of the simulation, the initiation of DNA unwrapping (inner DNA turn for H2A and outer turn for H3 tail), and the tail position during DNA detachment from the histone core. Both tails were located within the minor groove. However, while the H3 tail dissociated from the DNA upon unwrapping of the outer DNA turn, the H2A N-terminus remained associated with the DNA during the unwrapping of the inner DNA turn. Color coding: H2A, red; H2B, blue; H3, yellow; H4, green; DNA backbone, gray.
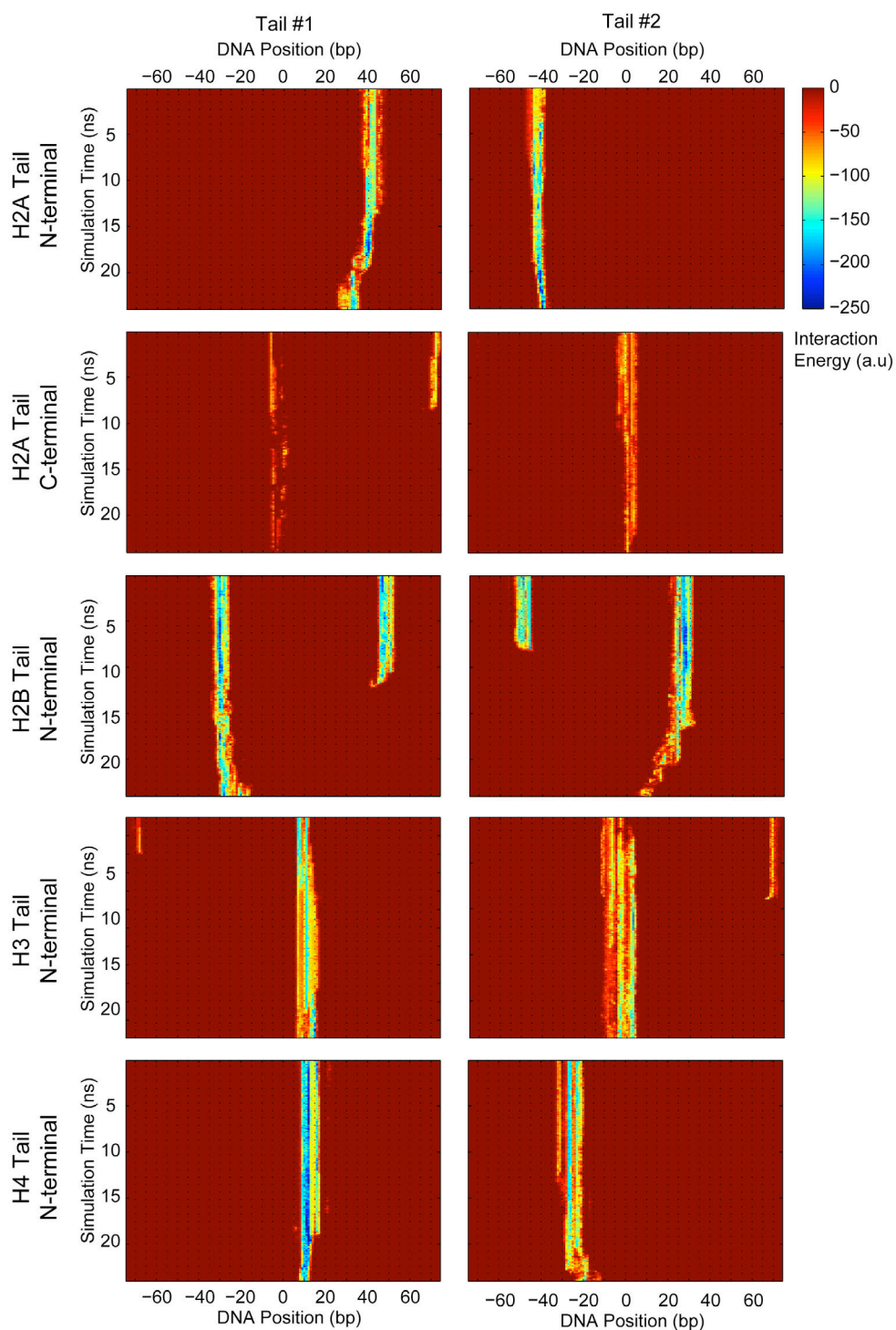
Figure S8. Histone H3 tails contribute to an increased stability of the inner DNA turn

For both nucleosomal copies of the indicated histone tails the time course of their DNA interactions during the SMD simulations is shown. Rearrangements of histone tails were visible in the N-terminal tails of H2A as well as H2B. However, only for the H3 tails the interaction with the inner turn increased after unwrapping the outer DNA turn. This transition occurred after approximately 4 ns (H3 tail #1) and 10 ns (H3 tail #2) of the SMD simulation. In contrast, both H4 tails displayed a continuous reduction of their DNA contacts.
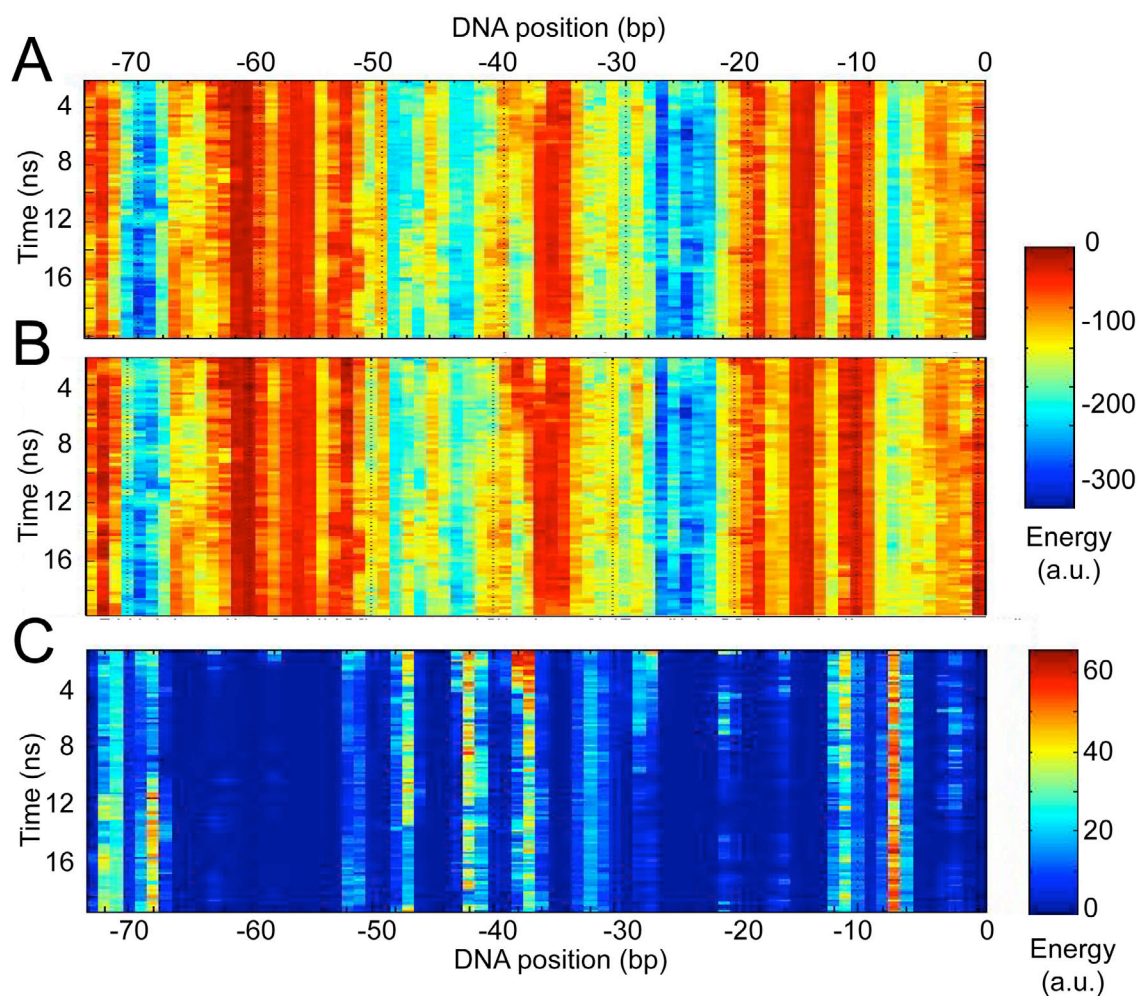
Figure S9. Analysis of DNA-DNA repulsion within the nucleosome

DNA-histone contacts according to the interaction energy color map over the course of the NUC MD simulations are shown for one half nucleosome (DNA position -73 to 0). (A) DNA-histone interactions without the contribution of DNA-DNA repulsion. (B) The interaction map including the DNA-DNA repulsion was almost the same as without DNA repulsion (color scale is the same as in top panel). (C) Isolated contribution of DNA-DNA repulsion energies. Note the difference in the relative energy scale.
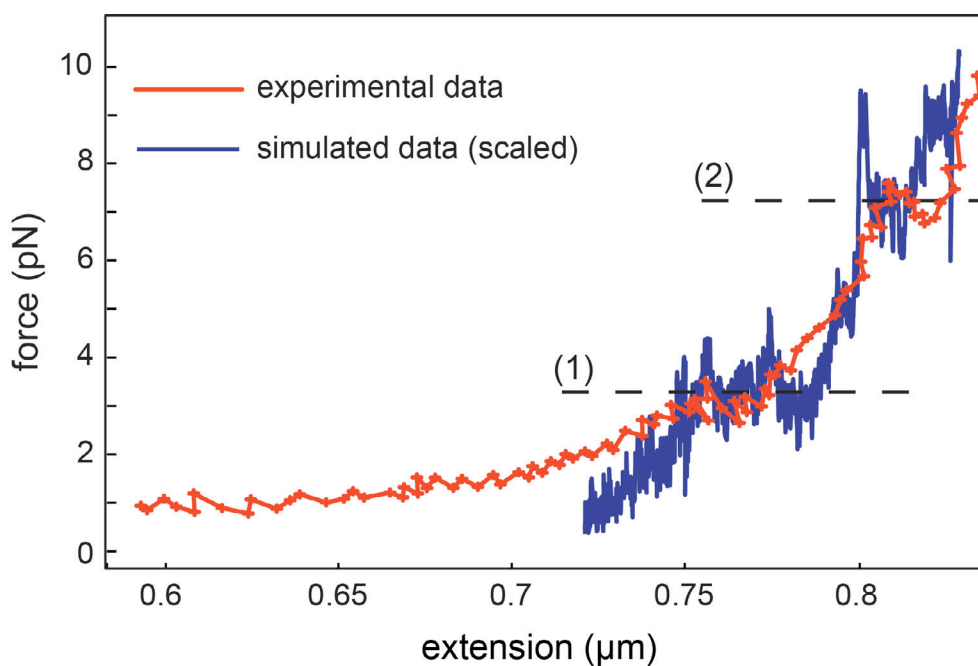
Figure S10. Comparison of simulated and experimental force spectroscopy curves of unwrapping DNA from the histone octamer

The shape of the scaled simulated curve is plotted in comparison to the experimentally observed transitions using the data set from ref. (12). The slope of the simulated data was somewhat steeper and fluctuations were more pronounced. The unwrapping of the outer DNA turn can be assigned to the plateau indicated by the dashed line at position 1 that was present in both the simulated and experimental curves. The second transition at position 2 comprised a complex overlay of contributions from the rearrangements and stretching of the DNA, as well as a partial opening of the histone octamer core in addition to further unwrapping of the inner DNA turn. This is concluded from the analysis of the SMD simulations.

Supplementary movie legends

Movie S1. Dynamics of a nucleosome with a central DNA loop.

MD simulation of the NUC_loop structure. The time step between each frame was 100 ps over a total period of 120 ns. Color code: H2B, olive; H2A, cyan; H3, yellow; H4, orange.

Movie S2. DNA unwrapping simulation of a complete nucleosome.

SMD simulation of the NUC structure. The time step between each frame was 20 ps over a total period of 24 ns. Color code: H2B, blue; H2A, red; H3, yellow; H4, green; DNA, light gray. DNA base pair -83 was fixed and a constant velocity force was applied at the C1' atom of DNA base pair +83.

Movie S3. DNA unwrapping simulation of a tailless nucleosome.

SMD simulation of the NUCΔtail structure. The time step between each frame was 40 ps over a total period of 20.2 ns. Color code and setup were as described in the legend to Movie S2.